ELSEVIER

Wear 210 (1997) 178–187

WEAR

Effects of a second phase on the tribological properties of Al_2O_3 and ZrO_2 ceramics

Y.J. He [a], A.J.A. Winnubst [a,*], D.J. Schipper [b], A.J. Burggraaf [a], H. Verweij [a]

[a] *Faculty of Chemical Technology, Laboratory for Inorganic Materials Science, University of Twente, P.O. Box 217, 7500 AE Enschede, The Netherlands*

[b] *Faculty of Mechanical Engineering, Laboratory of Tribology, University of Twente, P.O. Box 217, 7500 AE Enschede, The Netherlands*

Received 1 November 1996; accepted 16 December 1996

Abstract

The tribological properties of four different materials are investigated, tetragonal zirconia (Y-TZP), Al_2O_3 dispersed in Y-TZP (ADZ), ZrO_2 dispersed in Al_2O_3 (ZTA) and Al_2O_3 (with 300 ppm MgO). These materials are used as a cylinder sliding against a plate of Y-TZP (TZ-3Y)). Compared to Y-TZP, the wear resistance of ADZ composites is increased by a factor of 4–10. At a contact pressure of 230 MPa, a wear transition for Y-TZP is observed from plastic deformation to microchipping and microfracture due to the high interfacial temperature (450°C–550°C) generated by frictional heating. Because of the higher elastic modulus, hardness and fracture toughness at high temperature, ADZ composites show better wear resistance and a higher transition contact pressure (over 400 MPa) under the present conditions. For Al_2O_3, the transition from mild to severe wear occurs when the contact pressure is changed from 250 to 400 MPa. For ZTA ceramics, the wear behaviour does not change because of the presence of a compressive layer due to the zirconia phase transformation during sliding.

In water the wear resistance for ADZ and ZY5 is almost two orders of magnitude higher than the results under dry conditions. Reduction of the interfacial temperature by using water and the formation of a hydroxide layer at the contact surface by the tribochemical reaction of water with the ceramic, as observed by XPS, gives a positive effect on wear resistance.

Keywords: Ceramics; ZrO_2; AlO_2; Composites; Wear; Water influences; Surface analysis; XPS

1. Introduction

The use of advanced ceramics for wear applications has increased significantly in the last few years because of its high temperature capabilities and corrosion resistance. Although these properties are very promising, ceramics show catastrophic failure under stresses induced by thermal shock, erosion and wear processes because of their inherent brittleness.

In sliding wear, an initial period of mild wear can be followed by a transition to severe wear promoted by the formation of surface fractures [1,2]. As indicated by Hamilton et al. [3], large tensile stresses are formed at the rear of a sliding contact. Under certain conditions, the tensile stress at the tribological contact surface results in either crack propagation or brittle fracture. This causes a large friction coefficient and catastrophic or severe wear [4]. A number of studies has demonstrated that fracture plays a significant role in the wear process of ceramics [5–7]. Many attempts have been made to improve the fracture toughness of ceramic materials, and one of the most promising is the introduction of a second phase into the microstructure [8–10]. In particular, the use of metastable ZrO_2 particles or harder particles as a reinforcing element may improve wear resistance through the suppression of crack initiation and propagation. For example, the addition of ZrO_2 to an Al_2O_3 matrix results in a composite with a larger fracture toughness than single phase Al_2O_3 while maintaining the high hardness [11,12]. On the other hand, tetragonal zirconia materials have high values of strength and fracture toughness, making them competitive with metals for tribological applications. The wear resistance, however, is limited because of its relatively low hardness [13]. A dispersion of Al_2O_3 particles in a ZrO_2 matrix results in a ZrO_2–Al_2O_3 composite with higher hardness and elastic modulus. This composite may still maintain a high fracture toughness value. It has also been found that such materials have better high temperature mechanical properties by the addition of Al_2O_3 particles, because of crack deflection resulting in high fracture energies [14]. Composite ceramics combining the beneficial properties of either of the simple constituents can have good wear resistance because of their specially designed

* Corresponding author. Fax: 31534894683, E-mail: a.j-a.winnubst@ct.utwente.nl

0043-1648/97/$17.00
PII S0043-1648(96)07515-1

microstructure [15,16]. These composites seem to be potential materials for wear and mechanical applications under severe conditions [13].

The presence of water at the contact surfaces can significantly influence the wear rate of ceramic materials [17]. In some cases, when water acts as a coolant or lubricant, these effects are relatively straightforward [17–20]. In other cases, however, the water may interact chemically with the wear surface and facilitate degradation [21–25].

In this paper, the wear behaviour of ZrO_2, Al_2O_3, and their composites is described under defined conditions of constant load and sliding speed during sliding against a tetragonal zirconia plate. The tribological properties of the composites are investigated and compared. The influence of water as a lubricant on the wear behaviour of the different materials is also examined.

2. Experimental procedure

2.1. Wear test set-up and conditions

Wear tests were conducted employing a cylinder-on-plate type tribometer (S-tribometer) which consists of a cylinder with a diameter of 5.5 and 10 mm length of the test ceramic sliding with a sinusoidal velocity against a stationary plate of ZrO_2 ceramic (TZ-3Y). The apparatus for these tests and the specimen configuration are described in detail in Ref. [26]. All tests were performed at room temperature under two kinds of environmental conditions: ambient air with a relative humidity of about 50% or distilled water. The stroke of the reciprocating motion is 46 mm. All experiments were carried out at a frequency of 0.64 Hz which results in a mean velocity of 59 mm s^{-1} or a maximum velocity of 92.5 mm s^{-1}. Normal loads of 65 or 154 N were used. The corresponding initial Hertzian mean contact pressures, P, for both normal loads were calculated from [27]:

$$P=\frac{\pi}{4}\left(\frac{FE}{2\pi LR}\right)^{1/2} \quad (1)$$

where F is the normal load, L the contact length (in this case 10 mm) and E the equivalent Young's modulus as given by $1/E=1/2[(1-\nu_1^2)/E_1+(1-\nu_2^2)/E_2]$. ν_1,ν_2 and E_1,E_2 are, respectively, the Poisson ratios and the Young's moduli of the cylinder (1) and plate (2). R, the equivalent radius of curvature, is in this case 2.75 mm (line-contact). For a normal force of 65 N, the corresponding Hertzian contact pressure for the different materials is between 232 and 266 MPa. For a normal force of 154 N, the corresponding Hertzian contact pressure is between 356 and 409 MPa.

2.2. Materials investigated

The 4 different materials used as cylinder were: Y_2O_3 doped tetragonal ZrO_2, α-Al_2O_3, and two kinds of ZrO_2–Al_2O_3 composites. The compositions (and sample codes) of these materials were: ZrO_2–5 mol% $YO_{1.5}$ (=ZY5), ZY5–20 wt% (about 28 vol%) Al_2O_3 (=ADZ), Al_2O_3–15 wt% (about 10 vol%) ZrO_2 (=ZTA) and α-Al_2O_3 (with 300 ppm MgO). The preparation of ZY5, ADZ and ZTA are respectively given in the Refs. [28–30]. For the preparation of Al_2O_3, commercial available Al_2O_3 (Sumitomo AKP-50) was mixed with 300 ppm MgO by wet milling in ethanol. After isostatic compaction and sintering, all these ceramics had a relative density of more than 98%. All specimens were annealed (at 1000°C per 30 min for ZY5, and at 1300°C per 30 min for the other three materials) to remove the mechanical stress caused by machining and polishing. The surface roughness, R_a, was less than 30 nm. As the counter-plates TZ-3Y (TOSOH) ceramics, with a density of 99%, were used for all tests. The dimensions of the plate specimen were $56\times18\times8$ mm^3. After polishing, the surface roughness was less than 50 nm.

2.3. Characterization

The grain size was determined using the linear intercept technique [31]. The fracture toughness was measured by a three-point single-edge notched beam (SENB) technique. The Vickers hardness of the ceramics was measured by a micro-indenter (DUH-200 Shimadzu dynamic ultra hardness tester) with a load of 2 N. The surface roughness of the specimens was measured with a profilometer (Dek-Tak 3030). The worn tracks were observed by SEM (JSM-35CF, JEOL). The phase composition of the wear debris after sliding wear was examined by X-ray diffraction with Cu Kα radiation (Philips, PW 1710 diffractometer). The volume fraction of monoclinic zirconia was determined by Toraya's equation [32]. Adhesive particles on the worn surface were analysed using the energy dispersive X-ray (EDX) technique. The worn surface after wear tests in water was analysed by means of X-ray photoelectron spectroscopy (XPS). XPS measurements were performed using a Kratos XSAM-800, where Mg Kα radiation (1253.6 eV) was used to generate photoelectrons at a constant pass energy of 20 eV (FAT mode). The instrument was calibrated using the Ag $3d_{5/2}$, Cu $2p_{3/2}$ and Au $4f_{7/2}$ peaks.

3. Experimental results

3.1. Materials characteristics

Several properties of the materials used for tribological tests are given in Table 1. It should be noted that although the addition of Al_2O_3 to ZrO_2 (ADZ) has little or no effect on K_{IC} at room temperature, the hardness and elastic modulus are substantially increased about 15% compared to ZY5. For ZTA, the fracture toughness was increased about 30% if compared to alumina, while the hardness remained at a high value.

Table 1
Material properties of ZrO_2, Al_2O_3 and ZrO_2–Al_2O_3 composites

Material	ZY5	ADZ	ZTA	Al_2O_3	TZ-3Y
ZrO_2 grain size (μm)	0.33	0.3	0.3	–	0.33
Al_2O_3 grain size (μm)	–	0.4	0.8	1.8	–
Density, ρ (g cm^{-3})	5.90	5.44	4.15	3.92	6.00
Hardness, Hv (GPa)	13	15	18	19	13
Fracture toughness, K_{IC} (MPa m$^{1/2}$)	8.5	7.9	5.2	4.0	8.7
Young's modulus, E (GPa) [a]	210	253	370	392	210

[a] Data taken from Ref. [13].

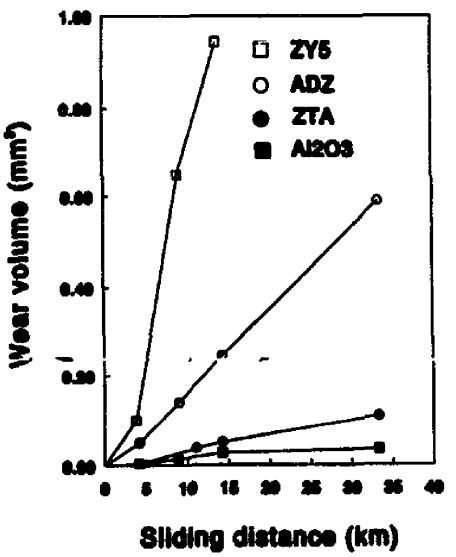

Fig. 1. Wear volume as a function of sliding distance in air for different ZrO_2 and Al_2O_3 composites. A normal load of 65 N is used.

3.2. Sliding wear under dry conditions

3.2.1. Wear of cylinder

At a normal load of 65 N, the wear volume of all specimens as a function of sliding distance is plotted in Fig. 1. The wear volume is calculated by the measured weight loss and the material density. After approximately 4 km of sliding distance, the wear of the ceramics tends to a constant wear rate with further sliding. The wear rates K, which are derived from the measured wear volumes ΔV, sliding distance s and applied load F, ($K=\Delta V/Fs$) are shown in Table 2. The values given in this table are average results (three measurements) within a deviation of ± 15% for all ceramics. A very important aspect of the wear results is the comparison of the wear rate of composite materials with those of single phase ZrO_2 and Al_2O_3. Under identical conditions, ADZ composites with a dispersed harder alumina phase show a significantly lower wear rate, i.e. higher wear resistance than ZY5. Wear rates of ZY5 for unlubricated sliding at room temperature are 1.30×10^{-6} and 31.1×10^{-6} mm^3 N^{-1} m^{-1} for normal loads of 65 and 154 N, respectively. These values are a factor of 4–6 higher than for ADZ. The change in the wear rates with increasing normal loads can clearly be seen in Fig. 2. The examination of wear debris obtained from ZY5/TZ-3Y and ADZ/TZ-3Y pairs by XRD indicates that no monoclinic zirconia phase is present. This means that no (irreversible) transformation of tetragonal zirconia takes place in ZY5, ADZ and TZ-3Y ceramics.

A comparison of the wear rates of ZTA and Al_2O_3 ceramics shows that ZTA reveals a slightly higher wear rate than Al_2O_3 at a normal load of 65 N (contact pressure, P, approximately 250 MPa). But at a high load of 154 N ($P\approx400$ MPa), ZTA ceramics show a significantly lower wear rate than Al_2O_3. The specific wear rate of Al_2O_3 is 1.44×10^{-6} mm^{-3} N^{-1} m^{-1}. This result is one order of magnitude larger than the wear rate of ZTA, and also almost one order of magnitude higher than the value obtained at the lower load (65 N). Upon changing the contact pressure from 250 to 400 MPa, the wear rate of ZTA remains almost constant, as shown in Fig. 2. XRD measurements indicate some monoclinic zirconia in the wear debris of the ZTA/TZ-3Y pair, but not in the wear debris of the Al_2O_3/TZ-3Y pair. No monoclinic zirconia phase is found on the worn surfaces of all TZ-3Y plates. The monoclinic zirconia phase in the wear debris of ZTA/TZ-3Y pair thus comes from the ZTA specimens.

3.2.2. Wear of TZ-3Y plate

The wear results of TZ-3Y plates worn by the four different types of ceramic cylinders are also given in Table 2. These results show that the wear rate of the plate depends on the cylinder materials and the normal forces. At a contact pressure of 250 MPa, the wear rate of the plate in the ADZ/TZ-

Table 2
Dry wear and friction properties of sliding wear of different ceramic cylinders on TZ-3Y plates

Sample composition	Normal load (N)	Specific wear rate K of cylinder (10^{-6} mm^3 N^{-1} m^{-1})	Specific wear rate K of plate (10^{-6} mm^3 N^{-1} m^{-1})	Friction coefficient f_c
ZY5	65	1.30	2.30	0.68
ADZ	65	0.29	1.80	0.60
ZTA	65	0.05	0.19	0.68
Al_2O_3	65	0.02	0.10	0.67
ZY5	154	31.10	34.70	0.70
ADZ	154	5.40	78.80	0.76
ZTA	154	0.08	0.50	0.76
Al_2O_3	154	1.44	3.80	0.71

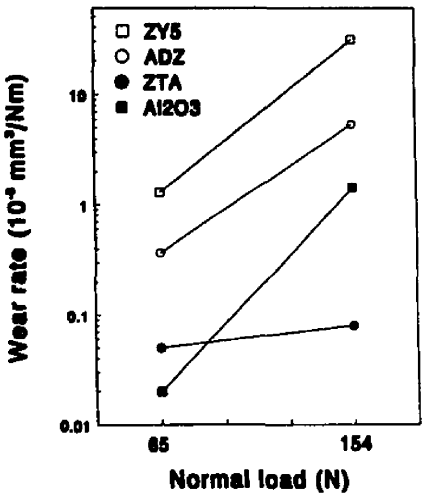

Fig. 2. Effect of normal loads on the wear rates of composite materials in air. Sliding distance is 15 km.

3Y pair is slightly lower than that in the ZY5/TZ-3Y pair. The wear rates of the plates in both the ZTA/TZ-3Y and the Al_2O_3/TZ-3Y pairs are almost the same, and are much lower than those in the ZY5/TZ-3Y and the ADZ/TZ-3Y pairs. At a higher contact pressure of 400 MPa, the wear rate of the plates in the ADZ/TZ-3Y pair is much higher than that obtained in the ZY5/TZ-3Y pair. The lowest wear rate of the plate at high pressure is again found for ZTA/TZ-3Y pair (note: this was also the case for the cylinder) despite the relative large friction coefficient. Compared to the ZTA specimen, the results show that using an Al_2O_3 specimen sliding against a TZ-3Y plate results in larger damage of the plate under the same loading conditions. No monoclinic zirconia phase was found on the worn surfaces of TZ-3Y plates using XRD examination.

3.2.3. Friction coefficients

The friction coefficients measured in these tests are listed in Table 2. At a normal load of 65 N, the values are in the range of 0.60–0.68, and at the higher loading force (154 N), the values are 0.70–0.76. There is a trend towards higher values at higher loads for all tested couples especially for the composite systems. Upon changing the contact pressures from 230 to 410 MPa, the friction coefficient slightly increases for the ADZ and ZTA while almost no change was observed for ZY5 and Al_2O_3 couples with Y-TZP.

3.3. Sliding wear in water

The effect of an aqueous environment on the wear behaviour was investigated at room temperature in distilled water. friction and wear results are summarized in Table 3. The mean specific wear rates of these experiments are given with an accuracy of ± 15%. The average friction coefficients show a scatter of ± 20%. For the four materials, in water environment, the friction coefficient is slightly decreased in comparison with the results obtained under dry conditions. In water, the ZY5 and ADZ ceramics have wear rates of 0.54×10^{-7} and 0.42×10^{-7} $mm^3\ N^{-1}\ m^{-1}$, respectively. These values are almost one order of magnitude lower than those under dry conditions (Table 2). For ZTA and Al_2O_3, water as a medium in the interface does not give a beneficial effect, and the wear rates even slightly increase compared to those under dry conditions. In addition, it is interesting to mention that the specific wear rates of the four ceramics are almost identical when sliding in water, while sliding under dry conditions, using the same conditions (load of 65 N) results in wear rate values which differ more than a factor 4.

3.4. Morphology of the wear track

3.4.1. Under dry conditions

Examination of the worn surfaces of the cylindrical specimens gives an indication for the wear mechanisms occurred. For ZY5 ceramics, under a normal load of 65 N, a mixture of rough and relatively smooth regions is observed in Fig. 3(a). The rough regions, which are very irregular and deeply grooved in the sliding direction, indicate a large degree of microfracture at the contact surface and in the subsurface. Accumulation of debris has already occurred on parts of the tracks. The small amount of smooth regions are characterized by plastic deformation (Fig. 3(b)). Observation of the wear track indicates that for ZY5 the transition from mild wear (plastic-deformation-controlled) to severe wear (microfracture-controlled) has started at a normal load of 65 N. Under a higher normal load of 154 N, all of the wear tracks show microfracture, as can be seen in Fig. 3(c). The higher degree of microfracture results in more wear debris adhering to the surface. Some areas in Fig. 3(d) show that large agglomerates of the debris are compacted and are smeared in the interface to form relatively dense and thick adhesive regions.

For ADZ ceramics, the wear track (Fig. 4(a)) reveals a very smooth surface under a normal load of 65 N. Little wear

Table 3
Friction and wear properties of different ceramic cylinders on TZ-3Y plates in water

Sample composition	Normal load (N)	Specific wear rate K of cylinder (10^{-7} $mm^3\ N^{-1}\ m^{-1}$)	Specific wear rate K of plate (10^{-7} $mm^3\ N^{-1}\ m^{-1}$)	Friction coefficient f_c
ZY5	65	0.54	0.89	0.60
ADZ	65	0.42	0.36	0.52
ZTA	65	0.68	0.42	0.52
Al_2O_3	65	0.41	1.04	0.61

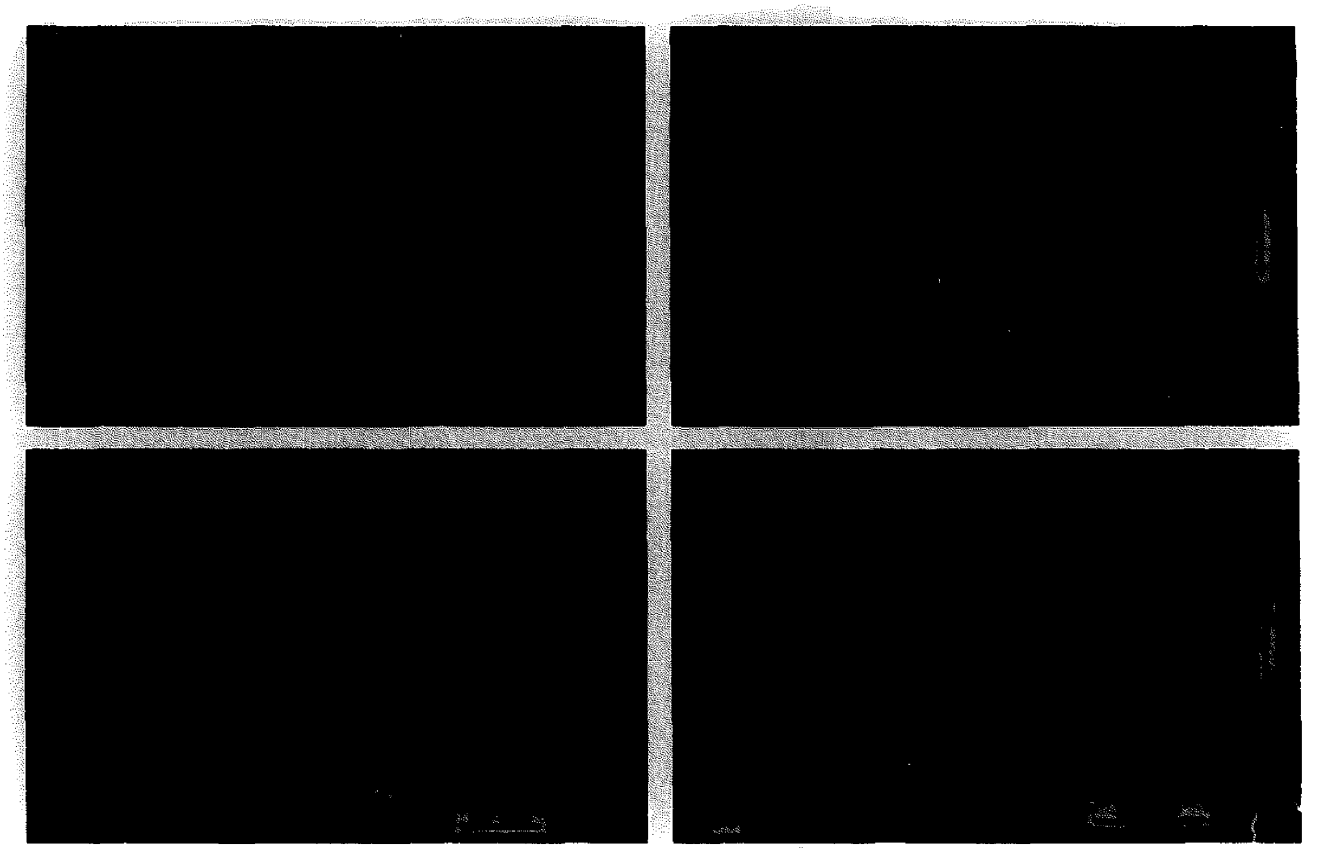

Fig. 3. Scanning electron micrographs of the worn surface of a ZY5 cylinder pin after sliding against a TZ-3Y plate in air (about 50% humidity). (a) and (b) show the wear tracks of ZY5 under a normal load of 65 N. (c) and (d) show the wear tracks of ZY5 under a normal load of 154 N. (a) Overview, (b) detail of the plastic deformation region, (c) overview of the wear track, (d) high magnification of (c). The arrows show the sliding direction of the counterface.

debris adheres to the material surface. In this material, no microcrack or microfracture is found at the contact surface. When a normal load of 154 N is used, the wear track shows a relatively thick and discontinuous adhered layer (Fig. 4(c)). This layer results from the compaction and shearing of large agglomerates of debris at the interface. At high magnification, the wear track shows less alumina particles (black particles in the SEM picture, Fig. 4(d)) in the debris (Fig. 4(d)) compared to bulk ADZ. This indicates that a large amount of wear debris came from the TZ-3Y plate, that is in agreement with the high wear rate (78.8×10^{-6} mm^3 N^{-1} m^{-1}) of the plate (Table 2). Along with the removal of the adhered debris, some grain pull-out of ADZ takes place during wear testing. In this case, no microcracks appear at the contact surface.

For ZTA ceramics at 65 N, the wear track shows a very smooth surface and some microfracture within very small areas (Fig. 5(a)). This means that wear of ZTA mainly is at a mild stage. A high magnification micrograph (Fig. 5(b)) shows some wear debris adhered to the surface of these microfractured regions. Under these tribological conditions, a high local tangential force is concentrated at the debris-rich areas resulting in either fracture at the surface flaws or grain pull-out accompanied with removal of wear debris. After sliding wear under the high normal load of 154 N, the wear track does not exhibit any difference from that under the normal load of 65 N.

For Al_2O_3 ceramics, under a normal load of 65 N, the wear track is very smooth, as shown in Fig. 6(a). Observation of the wear track at higher magnification (Fig. 6(b)) indicates the presence of some grain boundary microcracks accompanied with plastic deformation. The wear path has not been severely worn. When a high loading force of 154 N is used, a severe worn surface (Fig. 6(c)) is observed. The wear track shows a very irregular fracture and a rough surface, which is dominated by brittle fracture. In this case, the material removal is more pronounced. Examination of this surface at high magnification reveals that intergranular fracture is the principal process for the removal of material in Al_2O_3 (Fig. 6(d)).

3.4.2. *In aqueous environment*

The friction coefficient is slightly reduced by the use of water as a lubricant. Different phenomena take place on the materials tested in water. Observation of the microstructure is focused on the different cylinder materials after sliding wear in water at room temperature and under a normal load of 65 N.

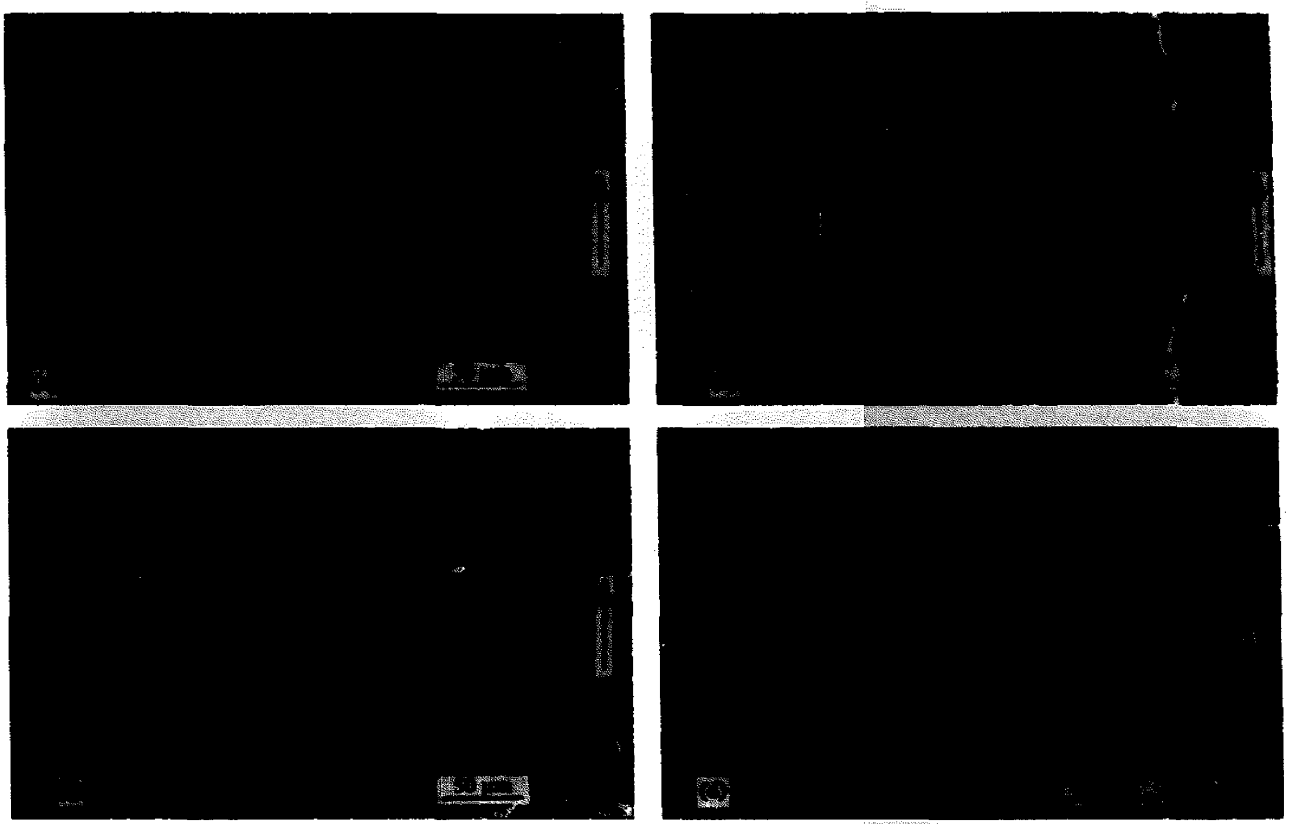

Fig. 4. Scanning electron micrographs of the worn surface of an ADZ cylinder pin after sliding against a TZ-3Y plate in air (about 50% humidity). Sliding wear under a normal load of 65 N; (a) overview of the wear track, (b) detail of the region with wear debris adhered on the surface. Sliding wear under a normal load of 154 N; (c) overview of the wear track, (d) high magnification of (c). The arrows show the sliding direction of the counterface.

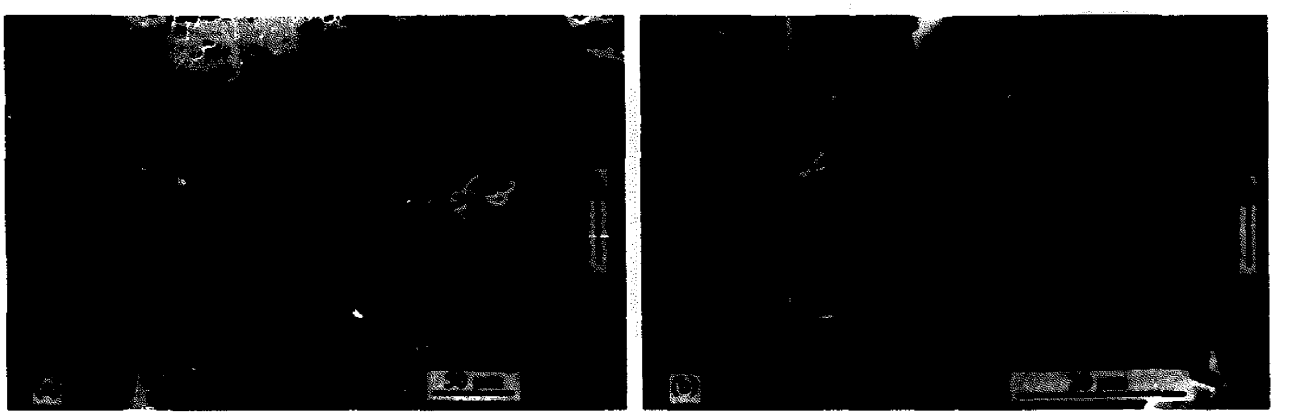

Fig. 5. Scanning electron micrographs of the worn surface of a ZTA cylinder pin after sliding against a TZ-3Y plate in air (about 50% humidity) under a normal load of 65 N; (a) overview of the wear track, (b) detail of the fracture region with some wear debris adhered to the surface.

The four ceramics tested in water show much smaller roughness values of wear surfaces than those of the samples tested in air. The worn surfaces of all these composites are very smooth. No microfracturing or microcracking occurred. The wear process of the materials is characterized by a fine polishing. Water prevents adhesion of wear debris to the surface, so debris is hardly observed in this case.

4. Discussion

4.1. Effects of material composition on wear

Under the circumstances investigated in this study the primary wear mechanisms in the four cylinder materials are considered to be plastic deformation and microfracture. The

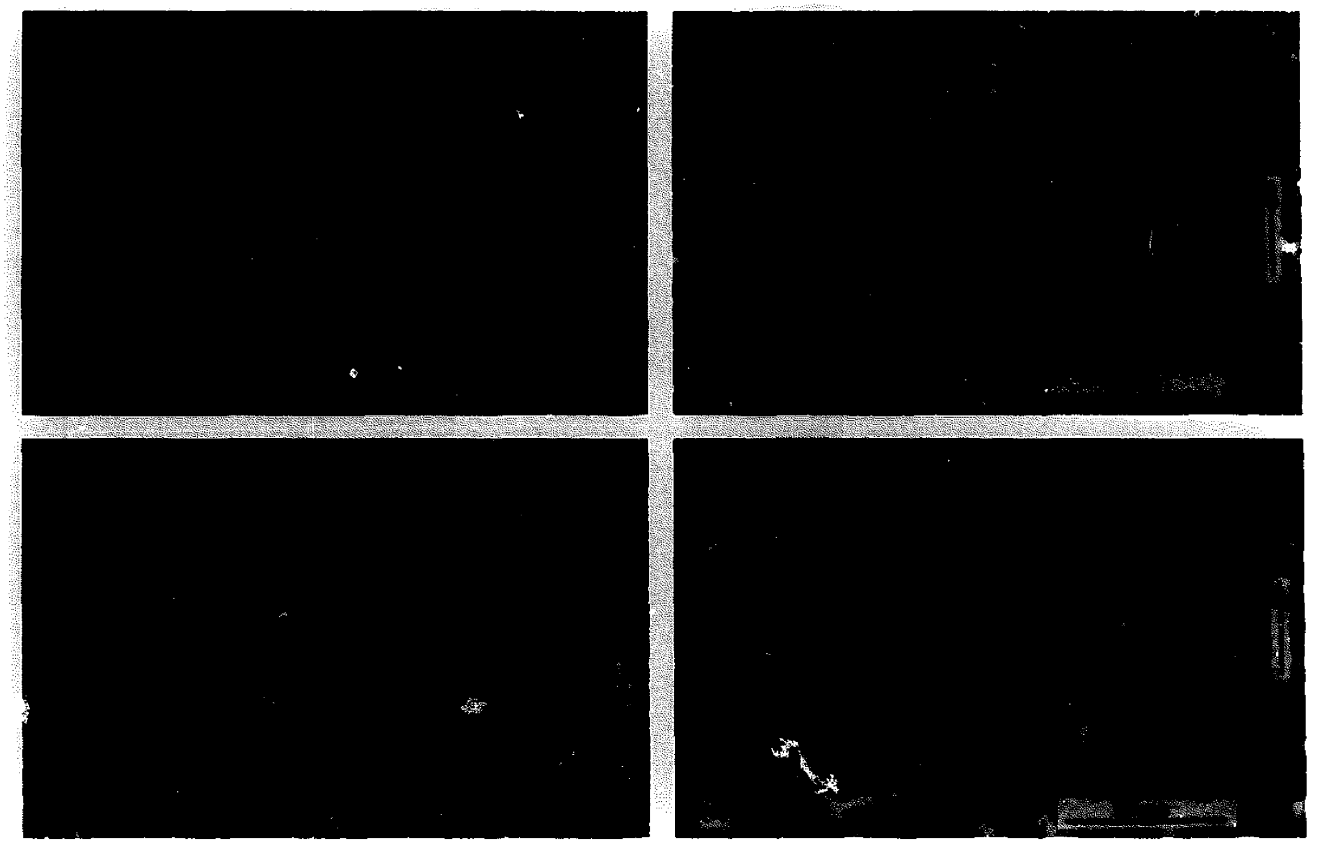

Fig. 6. Scanning electron micrographs of the worn surface of an Al_2O_3 cylinder pin after sliding against a TZ-3Y plate in air (about 50% humidity). Sliding wear under a normal load of 65 N: (a) overview of the wear track, (b) high magnification of (a). Sliding wear under a normal load of 154 N; (c) overview of the wear track, (d) high magnification of (c). The arrows show the sliding direction of the counterface.

change from a plastic-deformation-controlled wear to a brittle microfracture-controlled wear mechanism is generally accompanied by an increase in both friction coefficient and wear rate, i.e., a transition occurs from mild to severe wear [2].

At a normal load of 65 N, the wear loss of ZY5 is mainly caused by severe microfracture although some mild wear regions are still present. In this case, the transition to severe wear has taken place at or below this load. The wear resistance, is increased by addition of 20 wt% alumina particles in the ZY5 matrix (ADZ composite). At 65 N, the wear of ADZ composite is characterized by mild polishing with no microfracture. Even at a higher loading force of 154 N, the microfracture process is still not present. This indicates that under the present conditions, the normal load for wear transition in the ADZ composite is higher than 154 N.

The difference in wear resistance between ZY5 and ADZ composites under dry-sliding conditions depends on material properties such as fracture toughness, hardness, and also on the interfacial temperatures. Because of the low thermal conductivity of zirconia ceramics, a rapid temperature increase at asperities may be caused by frictional heating, and may play a role in the deterioration of these materials. For ZY5 ceramics, such a high temperature at the contact surface may result in three effects.

1. Large thermal stresses beneath the surface, i.e. at the subsurface layer by largely localized thermal gradients due to the poor thermal conductivity of ZrO_2.
2. Reduction of the fracture toughness at high temperature.
3. Development of thermal shock at local contact spots.

Due to these thermal processes microfracture at the subsurface can easily take place, especially in the area of internal volume defects such as flaws, voids, and weak grain boundaries. This results in a lower critical tensile stress for initiation and propagation of cracks and causes a wear transition at a relatively low loading force. At a higher load of 154 N, the higher surface temperature results in a further decrease in wear resistance. It is known that essentially all the mechanical work done to overcome friction is converted into heat and that this heat is generated in the immediate vicinity of the sliding interface. The value of the friction heat flux q is proportional to the friction coefficient μ, the normal force F, and the sliding velocity v, but inversely proportional to the nominal contact area A_n, as given by $q=\mu Fv/A_n$ [33]. Two temperatures are generated at the interface of contact materials by frictional heating. One is the bulk interfacial temperature, which under dry sliding could increase to a very high steady-state temperature controlled by for instance the geometry of the wear tester. The other temperature is the asperity temperature, generally referred to as the flash temperature,

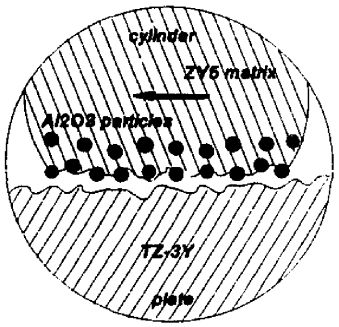

Fig. 7. Schematic representation of the presence of the harder alumina phase in ADZ sliding against a TZ-3Y plate.

which is generated in the local vicinity of asperity contact due to higher local heat fluxes. Using the temperature maps given by Ashby [33], both bulk and flash temperatures can be obtained. For a ZY5/TZ-3Y pair at a normal load of 65 N, the bulk interfacial temperature as well as the flash temperature reached values of about 450°C–550°C in this configuration. The surface temperature of ADZ composite cannot be calculated because some of the thermal properties are not known. The surface temperature is about 100°C–150°C for the Al_2O_3/TZ-3Y pair, which is lower than that in the ZY5/TZ-3Y pair because the thermal conductivity of Al_2O_3 (30 $W\,m^{-1}\,K^{-1}$) is larger than that of ZrO_2 (1.85 $W\,m^{-1}\,K^{-1}$). By increasing the normal load to 154 N, the surface temperature due to frictional heating increases to about 800°C and 200°C for ZY5 and Al_2O_3, respectively.

The multiphase ADZ material has a considerably better wear resistance in air than ZY5. This is due to the presence of the hard alumina particles, which increases the elastic modulus and the hardness of the system. The higher the hardness, the larger the resistance to abrasive wear. In this case, the relatively softer phase (ZrO_2 matrix) may plastically deform at the contact region. The hard alumina regions are exposed at the surface, as seen from the schematic representation in Fig. 7. As a result, good wear properties are obtained, i.e., wear is reduced because the Al_2O_3 particles protrude and become carrying regions. On the other hand, it has been mentioned that the effect of the interface temperature is predominant in ZY5 materials. For the ADZ composite, the interfacial temperature can be lower than in the ZY5. Even if the interfacial temperature reaches the same level as in the ZY5, the high fracture toughness is still remained due to the hard alumina particles providing microcrack deflection toughening, which is insensitive to temperature. Strengthening of zirconia materials at high temperatures by the addition of Al_2O_3 has been confirmed by Shi et al. [14]. In addition Trabelsi et al. [13] indicated that the high elastic modulus in ZrO_2–Al_2O_3 composites, and the stress applied by alumina particles to zirconia grains may lead to less dependence of K_{IC} on temperature. As a result of these higher fracture toughness and hardness values at higher temperature, the resistance to initiation and propagation of cracks is much higher than for ZY5. Finally this leads to a higher wear resistance in ADZ than in ZY5 if the influence of bulk/flash temperature on wear is high.

Although the ADZ composite shows a lower wear loss, the wear debris containing hard alumina particles result in stronger wear of the TZ-3Y counter plate by abrasive wear, especially under a high loading force of 154 N (see Table 2).

The best results (lowest wear rate) are observed for ZTA ceramics. It can be seen from Fig. 2 that the wear rate of ZTA ceramics is nearly constant by changing the normal load from 65 to 154 N, while the wear rate of Al_2O_3 strongly increases. The observations by scanning electron microscopy as described in Section 3.3 indicate that a wear transition from mild (plastic-deformation-controlled) to severe wear (brittle-fracture-controlled) has taken place for Al_2O_3 when the normal load changes from 65 to 154 N. For ZTA the critical load for wear transition is higher than 154 N. A transition from mild to severe wear occurs in brittle materials when the tensile stress at the contact exceeds a critical value for initiating fracture wear. This indicates that for ZrO_2 distributed in an Al_2O_3 matrix (ZTA), the critical tensile stress σ_D required for microcracks to propagate is enhanced in comparison with single phase Al_2O_3 ceramics. The critical tensile stress, σ_D, at which a crack propagates is calculated by the equation of Wang et al. [2]:

$$\sigma_D = \sigma_I^* \left(\frac{d^*}{d}\right)^{1/2} - \Sigma\sigma_{Ii} \qquad (2)$$

$\Sigma\sigma_{Ii}$ is the summation of internal stresses retained after thermal processing and the compressive stress resulting from the tetragonal to monoclinic zirconia phase transformation. Compressive stresses are represented with a negative sign. At the critical grain size $d = d^*$, $\Sigma\sigma_{Ii}$ reaches σ_I^* resulting in spontaneous microfracture at $\sigma_D = 0$. It is clear that enhancement of the microfracture resistance of ceramics at the contact surface can be achieved by refining the grain size and/or introducing an internal compressive stress. In ZTA composites the dispersion of zirconia reduces the mean alumina grain size (0.8 μm). Another factor which increases the wear resistance in ZTA compared to Al_2O_3 is the compressive residual stress induced by the ZrO_2 phase transformation on the surface of these materials. XRD analysis shows that a certain amount of tetragonal zirconia in ZTA has transformed to the monoclinic phase after sliding wear. A compressive layer is formed at the contact surface in ZTA, which leads to the increase in the critical tensile stress for initial propagation of cracks.

It is very important to mention that the presence of wear debris adhered to the surface in localized regions deteriorates the material properties because the local contact stress is concentrated at the wear debris area and hence much larger. These high local stresses result in crack propagation near and/or beneath the wear debris regimes. Fatigue processes due to repeated contact in these regimes lead to microfracture or grain pull-out.

4.2. Influence of water on wear behaviour

Sliding experiments of four materials were performed in distilled water. In order to investigate friction and wear behaviour of these materials in lubricated systems, it is necessary to know the lubrication conditions. Generally, three regimes are distinguished: full-film lubrication (HL), mixed lubrication (ML) and boundary lubrication (BL) [34]. For practical applications it is preferred that the tribosystem is under the HL or ML conditions. For determining the tribological properties and for understanding the tribochemical reaction during sliding wear in a water environment, the tribosystem must be in the boundary-lubricated region. Based on the operational conditions it is concluded that all tests are performed in the boundary-layer regime.

The experimental results show that the wear rates for ZY5 and ADZ are remarkably low in water, compared with dry sliding tests and only weakly dependent on composition. For ZTA and Al_2O_3, the wear rates do not change, but the morphologies of the worn surfaces are improved. After sliding tests in water, the worn surfaces are very smooth with no local microcracks or microfractures.

The discussions given above indicate that in air the flash temperature strongly influences the wear behaviour. In a water environment, the high interfacial temperature can be reduced. As a result, the thermal stresses in the subsurface area are reduced or even avoided. In this way, microchipping and microfracture are avoided. In addition, the smooth worn surface obtained in a water environment results in a relatively larger contact area and a more homogeneous stress distribution. This results in a reduction of the local contact pressure, and consequently decreases tensile stresses generated behind the moving cylinder. Tangential stresses may not be large enough to cause local microcracks on the surface by a recycle fatigue process. Therefore, the removal of material is reduced.

Another reason for the reduction in wear rate in a water environment is the formation of a hydroxide layer by a tribochemical reaction. The chemical structure of the contact surface has been analysed by XPS after sliding wear in water. In order to compare the result for the worn surface, polished specimens with no wear testing were also put in water for a certain time. Before XPS measurements, both specimens were cleaned ultrasonically in an ethanol bath and dried at 120°C. Fig. 8 shows the O 1s region of the XPS spectrum performed on the surfaces. The XPS spectra for the polished specimens show a main signal at a binding energy of 530–531 eV which is ascribed as zirconium in the oxide form (Fig. 8(a)). The XPS spectra of the worn surface after sliding wear in water show a shoulder at a binding energy of 532–533 eV (Fig. 8(b)). This extra signal can be ascribed as the O–OH, Y–OH or Zr–OH binding forms. This result indicates the formation of a hydroxide layer or of chemically adsorbed water after wear. In this case, the lubricant effects become beneficial because this layer possesses some solid lubricating ability [20] or can prevent direct contact of the surfaces, resulting in a reduced specific wear rate. The hydroxide layer or the chemically adsorbed water also reduce the friction coefficients by reduction of shear strength of contact surface. The positive effects of water on the wear resistance of ceramics are also confirmed by other investigators, who found that the wear rate is remarkably reduced by the formation of a hydrated layer in alumina ceramics [17–19].

As mentioned by Sato et al. [35] the process of chemisorption and diffusion of OH^- ions to ZrO_2 lattice is time dependent, so it is not clear whether wear damage is accelerated by the degradation of ZrO_2 ceramic properties after prolonged sliding. If water still gives a positive effect after prolonged sliding, it is still not easy to state which role of water is predominant, the cooling action or the formation of a hydroxide layer.

5. Conclusions

Compared to single phase ZY5, the wear resistance of ADZ composites with 20 wt% Al_2O_3 dispersed in a ZY5 matrix is increased by a factor of 4–10.

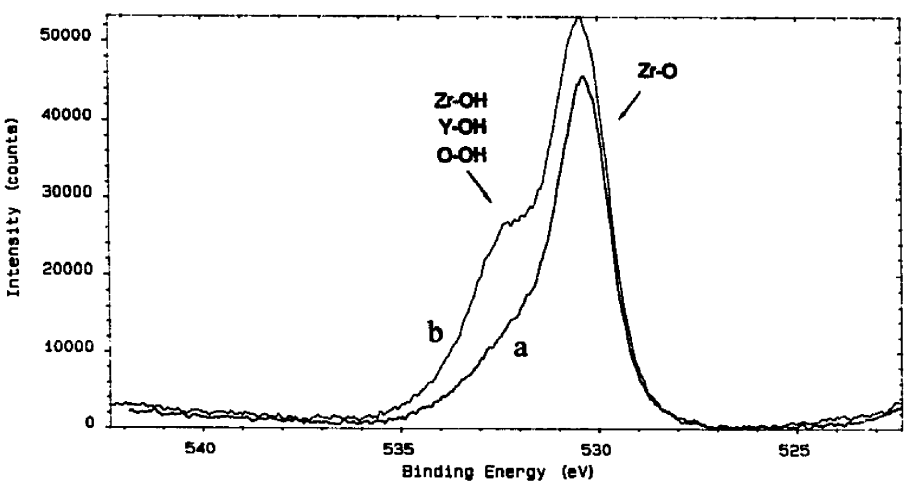

Fig. 8. XPS spectra for the O 1s region of TZ-3Y, (a) polished surface before sliding wear; (b) worn surface after sliding wear in water.

Under a normal load of 65 N (Hertzian contact pressure approximately 250 MPa), the wear mechanism for ZY5 undergoes a transition from plastic deformation to microchipping and microfracture. The high interfacial temperature (450°C–550°C) generated by friction heating results in the introduction of thermal stresses at the subsurface, ultimately reducing the wear resistance. Upon increasing the normal load to 154 N (Hertzian contact pressure approximately 400 MPa), the wear rate of ZY5 ceramics is increased by approximately two orders of magnitude due to the higher contact pressure resulting in a higher interfacial temperature. Because of the higher elastic modulus and hardness, ADZ composites show a better wear resistance and a higher transition load (over 154 N). The wear rate of ADZ is increased by approximately one order of magnitude with a change in the normal load from 65 to 154 N due to more grain pull-out, but wear is still in a mild stage.

Under a normal load of 65 N, the wear rate of Al_2O_3 ceramics is slightly lower than that of ZTA ceramics, but under a normal load of 154 N, the wear rate of ZTA ceramics is much lower than that of Al_2O_3. For Al_2O_3 ceramics, the transition from mild to severe wear occurs when the normal load is changed from 65 to 154 N; this is not the case for ZTA ceramics. For ZTA ceramics, the wear behaviour is improved by the presence of a compressive layer due to the zirconia phase transformation during sliding and by the relative small alumina grain size.

In water environment, the friction and wear behaviour of all composite ceramics tested are improved, especially for ADZ and ZY5, for which the wear rates are almost one or two orders of magnitude less than under dry conditions. The high interfacial temperature can be reduced by water. As a result of the reduction in the temperature, microcracks and microfractures are avoided at the contact surface or subsurface. The formation of a hydroxide layer at the contact surface by tribochemical reaction of water with the ceramic also gives a positive effect on the wear resistance.

References

[1] L.D. Wedeven, R.A. Pallini, N.C. Miller, in: K.C. Ludema (Ed.), Wear of Materials, Am. Soc. Mech. Eng., New York, 1987, pp. 333–347.
[2] Y.S. Wang, C. He, B.J. Hockey, P.I. Lacey, S.M. Hsu, Wear 181–183 (1995) 156–164.
[3] G.M. Hamilton, L.E. Goodman, J. Appl. Mech. 6 (1966) 371–376.
[4] S.M. Hsu, Y.S. Wang, R.G. Munro, Wear 134 (1989) 1–11.
[5] M.V. Swain, Wear 35 (1975) 185–189.
[6] N.S. Eiss, R.C. Fabiniak, J. Am. Ceram. Soc. 49 (1966) 221–226.
[7] C.S. Yust, F.J. Carignan, ASLE Trans. 28 (1985) 245–252.
[8] P.F. Becher, G.C. Wei, Commun. Am. Ceram. Soc. 67 (1984) 259–260.
[9] G.C. Wei, P.F. Becher, Am. Ceram. Soc. Bull. 64 (1985) 298–304.
[10] R.C. Garvie, R.H. Hannink, R.T. Pascoe, Nature 258 (1975) 703–704.
[11] P.F. Becher, T.N. Tiegs, J. Am. Ceram. Soc. 70 (1987) 651–654.
[12] T.N. Tiegs, P.F. Becher, Ceramic materials and components for engines, in: Proceedings of the Second International Symposium, Lubeck-Travemunde, Germany, April 14–17, 1986, pp. 193–200.
[13] R. Trabelsi, D. Treheux, G. Orange, G. Fantozzi, Tribol. Trans. 1 (1989) 77–84.
[14] J.L. Shi, B.S. Li, T.S. Yen, J. Mater. Sci. 28 (1993) 4019–4022.
[15] C. He, Y.S. Wang, J.S. Wallace, S.M. Hsu, Wear 162–164 (1993) 314–321.
[16] C.S. Yust, Tribology of composite materials, in: P.K. Rohatgi, P.J. Blau, C.S. Yust (Eds.), Proceedings of a Conference, Oak Ridge, TN, 1–3 May, 1990, pp. 25–33.
[17] J.E. Hines, Jr., R.C. Bradt, J.V. Biggers, Tribology of composite materials, in: P.K. Rohatgi, P.J. Blau, C.S. Yust (Eds.), Proceedings of a Conference, Oak Ridge, TN, 1–3 May, 1990, pp. 540–50.
[18] S. Sasaki, J. Soc. Lubric. Eng. Jpn. 33 (1988) 620–28 (in Japanese).
[19] J.E. Hines, Jr., R.C. Bradt, J.V. Biggers, in: W.N. Gleaser, K.C. Ludema, S.K. Rhee (Eds.), Wear of Materials, Am. Soc. Mech. Eng., New York, 1977, pp. 462–467.
[20] R.S. Gates, S.M. Hsu, E.E. Klaus, Tribol. Trans. 32 (1989) 357–63.
[21] A.G. Evans, J. Mater. Sci. 7 (1972) 1137–46.
[22] T.A. Michalske, B.C. Bunker, S.W. Freiman, J. Am. Ceram. Soc. 69 (1986) 721–24.
[23] T.E. Fischer, W.M. Mullins, Chemtech (1993) 27–31.
[24] T. Kawakubo, H. Hirayama, A. Goto, T. Kaneko, J. Soc. Mater. Sci. Jpn. 38 (1989) 300–306.
[25] S. Kitaoka, Y. Yamaguchi, Y. Takahashi, J. Am. Ceram. Soc. 75 (1992) 3075–80.
[26] Y.J. He, A.J.A. Winnubst, D.J. Schipper, P.M.V. Bakker, A.J. Burggraaf, H. Verweij, Wear 184 (1995) 33–43.
[27] D. Bialo, J. Duszczyk, A.W.J. de Gee, G.J.J. van Heijningen, B.M. Korevaar, Wear 141 (1991) 291–309.
[28] W.F.M. Groot Zevert, A.J.A. Winnubst, G.S.A.M. Theunissen, A.J. Burggraaf, J. Mater. Sci. 25 (1990) 3449–3455.
[29] P.M.V. Bakker, Y.J. He, A.J.A. Winnubst, A.J. Burggraaf, H. Verweij, in: H. Hausner, G.L. Messing, S.-I. Hirano (Eds.), Ceramic Processing Science and Technology, Ceramic Transactions, vol. 51, Am. Ceram. Soc., OH, 1995, pp. 537–541.
[30] P. Den Exter, A.J.A. Winnubst, T.H.P. Leuwerink, A.J. Burggraaf, J. Am. Ceram. Soc. 77 (1994) 2376–2380.
[31] M.I. Mendelson, J. Am. Ceram. Soc. 52 (1969) 443–46.
[32] H. Toraya, M. Yoshimura, S. Sōmiya, J. Am. Ceram. Soc. 67 (1984) C119–C121.
[33] M.F. Ashby, J. Abulawi, H.S. Kong, T-Maps, University of Cambridge, Engineering Dept., 1990.
[34] D.J. Schipper, A.W.J. de Gee, ASME J. Tribol. 117 (1990) 250–254.
[35] T. Sato, M. Shimada, J. Am. Ceram. Soc. 68 (1985) 356–359.